Pseudorapidity dependence of parton energy loss in relativistic heavy ion collisions

Tetsufumi Hirano[1] and Yasushi Nara[2]
[1]*RIKEN BNL Research Center, Brookhaven National Laboratory, Upton, New York 11973, USA*
[2]*Department of Physics, University of Arizona, Tucson, Arizona 85721, USA*
(Received 28 July 2003; published 4 December 2003)

We analyze the recent data from the BRAHMS Collaboration on the pseudorapidity dependence of nuclear modification factors in Au+Au collisions at $\sqrt{s_{NN}}$=200 GeV by using the full three dimensional hydrodynamic simulations for the density effects on parton energy loss. We first compute the transverse spectra at η=0 and 2.2, and next take a ratio $R_\eta = R_{AA}(\eta=2.2)/R_{AA}(\eta=0)$, where R_{AA} is a nuclear modification factor. It is shown that hydrodynamic components account for $R_\eta \simeq 1$ at low p_T and that quenched perturbative QCD components lead to $R_\eta < 1$ at high p_T which are consistent with the data. Strong suppression at η=2.2 is compatible with the parton energy loss in the final state.

DOI: 10.1103/PhysRevC.68.064902 PACS number(s): 24.85.+p, 25.75.−q, 24.10.Nz

Recent data from the Relativistic Heavy Ion Collider (RHIC) reveal that hadron spectra at high p_T in central Au+Au collisions are strongly suppressed relative to the scaled *pp* or large centrality spectra by the number of binary collisions [1–5] contrary to the enhancement in *d*+Au collisions [6–9]. The RHIC data are consistent with the early predictions on jet quenching due to gluon bremsstrahlung induced by multiple scattering [10] as a possible signal of deconfined nuclear matter, the quark gluon plasma (QGP) [11] (for a recent review, see Ref. [12]). Observed suppression of the away-side peak in dihadron spectra in central Au+Au collisions [13] is also considered to be due to jet quenching, while correlation spectra in *d*+Au collisions are the same as in *pp* collisions [7], where it is not expected to create hot and dense matter. Large elliptic flow observed in high-p_T region is also considered to be a consequence of jet quenching [14,15]. Phenomenological studies based on the parton energy loss [16–19] are successful in describing various high-p_T hadron spectra at RHIC: suppression of single particle spectra [20–23], suppression of away-side correlation [23,24], azimuthal anisotropy of high-p_T hadron spectra in noncentral collisions [23,25–27] including centrality dependences [23].

In addition to those data, the BRAHMS Collaboration recently reported the pseudorapidity dependence of the nuclear modification factors and showed that the yields of high-p_T charged hadrons are strongly suppressed even at η=2.2 [9]. Furthermore, it is also shown that the ratio $R_\eta^{CP} = R_{CP}(\eta=2.2)/R_{CP}(\eta=0)$, where R_{CP} is a ratio of central to most peripheral yields normalized by the number of binary collisions, is almost unity at $p_T < 2$ GeV/c and $R_\eta^{CP} < 1$ at high p_T. These data are the first results of high-p_T spectra in the forward rapidity region at RHIC and, thus, provide the novel opportunity to study how the dense matter is distributed in the longitudinal directions. Therefore, further systematic studies are necessary to confirm the presence of the jet quenching in the dense medium at RHIC. In this paper, we analyze p_T spectra at η=2.2 by employing the hydro+jet model [22,24,27,28] and test if the scenario of jet quenching in the QGP phase is still consistent with data.

Hydrodynamics is found to be successful for the description of the soft part of the matter produced in Au+Au collisions at RHIC especially in midrapidity region ($Y \simeq 0$) [29]. Motivated by these results, we also describe the space-time evolution of thermalized matter even in off-midrapidity region ($Y \neq 0$) by solving the equations for energy-momentum conservation in the *full* three-dimensional (3D) Bjorken coordinate (τ, x, y, η_s) [30,31]. Here $\tau = \sqrt{t^2 - z^2}$ is the proper time and $\eta_s = (1/2)\ln[(t+z)/(t-z)]$ is the space-time rapidity. Even at RHIC energies, one cannot observe "central plateau [32]" in the rapidity distribution [33] in Au+Au collisions. Note that a plateaulike structure in the *pseudorapidity* distribution observed at RHIC [34,35] simply comes from the Jacobian between rapidity and pseudorapidity. In addition, elliptic flow as a function of pseudorapidity shows a peak at midrapidity [36]. These data suggest that the full 3D hydrodynamic simulations are necessary for discussion on the global behavior in heavy ion collisions even at RHIC energies. Although our initial condition for longitudinal flow rapidity (defined as $Y_f = (1/2)\ln[(1+v_z)/(1-v_z)]$ where v_z is the longitudinal flow velocity) is still assumed to be the exact scaling solution $Y_f(\tau_0, x, y, \eta_s) = \eta_s$, we obtain the rapidity dependent observables by taking an η_s dependent initial energy density distribution which is factorized by a function

$$H(\eta_s) = \exp\left[-\frac{(|\eta_s| - \eta_{\rm flat}/2)^2}{2\eta_{\rm Gauss}^2} \theta(|\eta_s| - \eta_{\rm flat}/2) \right], \quad (1)$$

where $\eta_{\rm flat}$ and $\eta_{\rm Gauss}$ control the size of a flat (Bjorken-like) region near midrapidity and the width of Gaussian function in forward/backward rapidity, respectively [37]. The pseudorapidity distributions of charged hadrons in central and semicentral collisions observed by BRAHMS [34] are already reproduced by choosing $\eta_{\rm flat}/2 = 2$ and $\eta_{\rm Gauss} = 0.8$ and also by taking account of local rapidity shift at each transverse coordinate $\eta_{s0}(x, y)$ in Eq. (1) [27]. For details on how to parametrize initial conditions in our hydrodynamic model, see Ref. [31]. In hydrodynamic calculations, a partial chemical equilibrium model with chemical freeze-out temperature $T^{\rm ch} = 170$ MeV is employed for the hadronic phase to describe the early chemi-

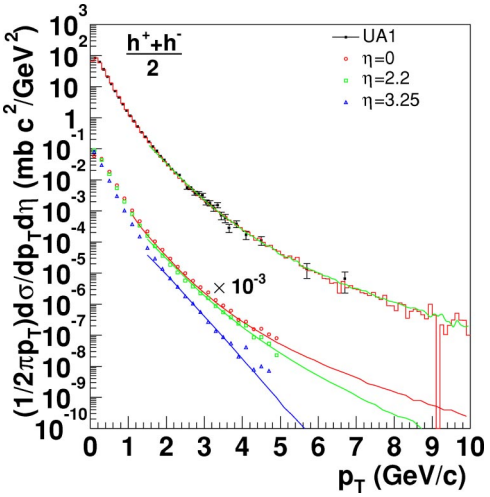

FIG. 1. (Color online) Invariant spectra of charged hadrons from UA1 data [41] in $p\bar{p}$ collisions at $\sqrt{s}$=200 GeV are compared to PYTHIA predictions with Lund fragmentation (histogram) and with independent fragmentation model (line). η dependence is also shown for both models. Circles, squares, and triangles correspond to the predictions from PYTHIA with Lund fragmentation at η =0, 2.2, and 3.25, respectively, which are compared to the results from PYTHIA with independent fragmentation model (lines).

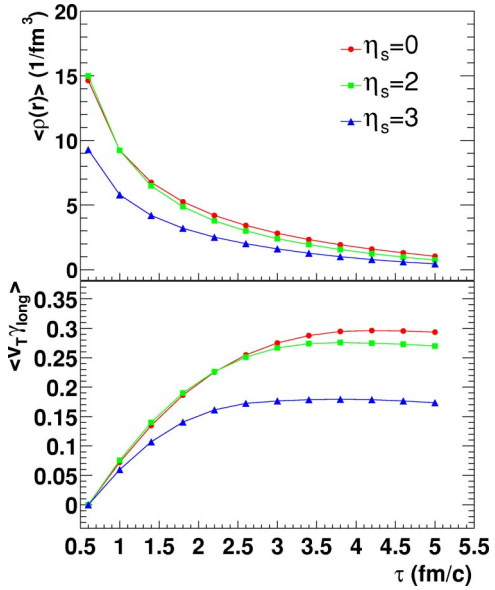

FIG. 2. (Color online) Time evolutions of average parton density (upper panel) and average $\gamma_{\rm long}$-weighted transverse velocity (lower panel) at space-time rapidity η_s=0, 2, and 3 from hydrodynamic simulations in 0–10% central Au+Au collisions at $\sqrt{s_{NN}}$ =200 GeV. Impact parameter is b=3.7 fm. Average is taken only in the QGP and mixed phases.

cal freeze-out picture of hadronic matter [31]. On the other hand, the QGP phase is assumed to be a massless free partonic gas with the number of flavors N_f=3.

For the hard part of the model, we generate hard partons according to a perturbative QCD (pQCD) parton model. We use PYTHIA 6.2 [38] for the generation of momentum spectrum of jets through 2→2 QCD hard processes. Initial and final state radiations are used to take into account the enhancement of higher-order contributions associated with multiple small-angle parton emission. The CTEQ5 leading order parton distribution function [39] is used. Hadrons are obtained from an independent fragmentation model option in PYTHIA. The K factor K=2.5, the scale $Q=p_{\rm T,jet}/2$ in the parton distribution function, and the primordial transverse momentum $\langle k_{\rm T}^2\rangle_{NN}$=1.2 GeV$^2/c^2$ are used to fit the neutral pion transverse spectrum in pp collisions at RHIC [40]. UA1 data [41] for charged hadrons are also well reproduced with these parameters in the transverse momentum range $p_{\rm T}>2$ GeV/c as shown in Fig. 1. Independent fragmentation model is not applicable for the low-$p_{\rm T}$ transverse momentum range. Hence we use the Lund string model for the pp reference when we compute nuclear modification factors at low $p_{\rm T}$($p_{\rm T}<2$ GeV/c). EKS98 parametrization [42] is employed to take into account the nuclear shadowing effect. The Cronin enhancement is modeled by the multiple initial state scatterings as in Ref. [43].

Initial transverse positions of jets are determined randomly according to the number of binary collision distribution. Initial longitudinal position of a parton is approximated by the boost invariant distribution [32]. Jets are freely propagated up to the initial time τ_0(=0.6 fm/c) of hydrodynamic simulations by neglecting the possible interactions in the prethermalization stages. Jets are assumed to travel with straight line trajectory in the medium.

Jets can suffer interaction with fluids and lose their energies. We employ the approximate first order formula (Gyulassy-Levai-Vitev formula) in opacity expansion from the reaction operator approach [19] for the energy loss of partons in this work. The approximate first order formula in this approach can be written as

$$\Delta E = C\int_{\tau_0}^{\infty} d\tau\rho(\tau,\boldsymbol{x}(\tau))(\tau-\tau_0)\ln\left(\frac{2E_0}{\mu^2 L}\right). \qquad (2)$$

Here we take L=3 fm and μ=0.5 GeV. C=0.45 is an adjustable parameter and $\rho(\tau,\boldsymbol{x})$ is a thermalized parton density in the local rest frame of fluid elements in the hydro +jet approach [44]. $\boldsymbol{x}(\tau)$ and E_0 are the position and the initial energy of a jet, respectively. The initial energy E_0 in Eq. (2) is Lorentz boosted by the flow velocity and replaced by $p_0^\mu u_\mu$ where p_0^μ and u_μ are the initial four-momentum of a jet and a local fluid velocity, respectively. The parameters related to the propagation of partons are obtained by fitting the nuclear modification factor for the neutral pion by PHENIX [2] and are found to be consistent [24] with the back-to-back correlation data from STAR [13].

Let us start with the study of the space-time rapidity dependence of transverse dynamics from the full 3D hydrodynamics. In order to understand the dynamical effects on parton energy loss, we plot in Fig. 2 parton densities and $\gamma_{\rm long}$-weighted transverse flow velocities averaged over the QGP and mixed phases as a function of τ at η_s=0, 2, and 3. Here a gamma factor of longitudinal flow is $\gamma_{\rm long}=\cosh(Y_{\rm f})$. Note that the quantity $\langle v_{\rm T}\gamma_{\rm long}\rangle$ is independent of the space-time rapidity η_s when the initial longitudinal flow and the

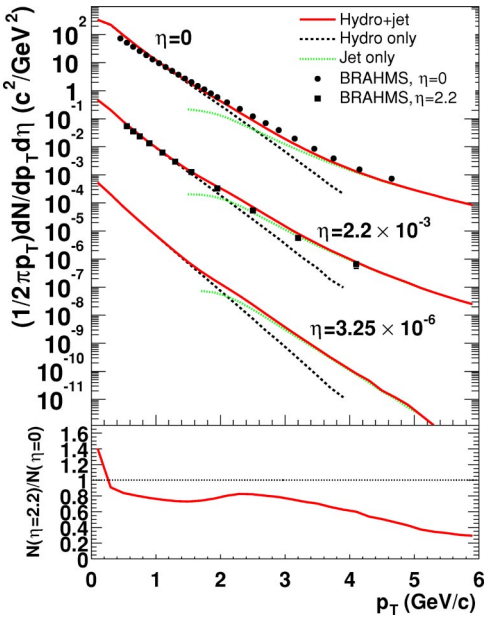

FIG. 3. (Color online) Transverse momentum distributions of charged hadrons in Au+Au collisions at $\sqrt{s_{NN}}$=200 GeV are compared to data from BRAHMS [9]. Solid lines represent the hydro +jet result averaged over $|\eta|<0.1$, $2.1<|\eta|<2.3$, and $3.0<|\eta|<3.5$. The impact parameter for 0–10% centrality is taken to be b=3.7 fm. In the bottom panel the ratio of the spectrum at η=2.2 to that of η=0 is plotted. Enhancement at very low p_T comes from the effect of Jacobian for the transformation of rapidity to pseudorapidity.

initial energy density obey the scaling solution $Y_f(\tau_0, x, y, \eta_s)=\eta_s$ and $e(\tau_0, x, y, \eta_s)=e(\tau_0, x, y)$, respectively. We note that longitudinal flow from full 3D hydrodynamics remains to be close to the Bjorken flow: $Y_f \approx \eta_s$ at $\eta_s<3$ within our initial conditions used in this work. As shown in the figure, the difference of the time evolutions of the thermalized parton density and the transverse flow velocity between η_s=0 and η_s=2 are practically tiny, since the initial scaling region reaches to $\eta_s=\eta_{flat}/2=2$ [45]. Thus, the dynamical effect on the jet energy loss at η=0 and 2.2 is expected to be the same, whereas the amount of jet energy loss at η=3 must be small because of the smaller parton density. As will be shown in Fig. 4, we should emphasize here that this does not mean $R_{AA}(\eta=0)\approx R_{AA}(\eta=2.2)$.

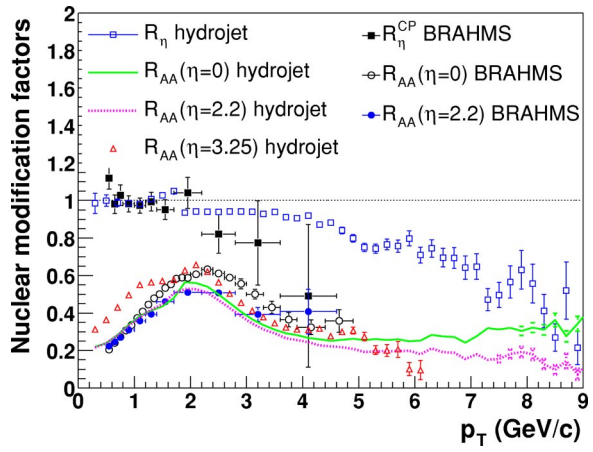

FIG. 4. (Color online) Nuclear modification factors are compared to the BRAHMS data [9] in Au+Au collisions at $\sqrt{s_{NN}}$ =200 GeV.

We next show in Fig. 3 the transverse momentum distributions for charged hadrons from the hydro+jet model in central Au+Au collisions at RHIC. Thermal freeze-out temperature T^{th}=100 MeV is used in the calculation. This choice is consistent with the PHENIX data at $\sqrt{s_{NN}}$=130 GeV [31]. Each spectrum is the sum of the soft component and the hard component. Before summation, the hard component is multiplied by a "switch" function [25] $\{1+\tanh[2(p_T-2)]\}/2$ (where p_T is in the unit of GeV/c) in order to cut the unreliable components from the independent fragmentation scheme and also to obtain the smooth spectra. The hydrodynamic components are dominated in the range of $p_T<2$ GeV/c. The slope of hadrons in low-p_T region at η =0 is nearly the same as the one at η=2.2 as clearly seen in the bottom panel of Fig. 3 in which the ratio of the spectrum at η=2.2 to that at η=0 is plotted. This results from the similarity of transverse dynamics between η=0 and 2 as shown in Fig. 2. On the other hand, the slope from pQCD components in high-p_T region becomes steeper as η increases, reflecting the original pp spectra (see Fig. 1).

We now turn to the study of the nuclear modification factors R_{AA} for charged hadrons defined by

$$R_{AA}=\frac{\dfrac{dN^{A+A}}{d^2p_T d\eta}}{N_{\rm coll}\dfrac{dN^{p+p}}{d^2p_T d\eta}}, \tag{3}$$

where $N_{\rm coll}$ is the number of binary collisions. Figure 4 shows the nuclear modification factors R_{AA} for charged hadrons at η=0, 2.2, and 3.25 in Au+Au collisions at RHIC for an impact parameter b=3.7 fm. The nuclear modification factors R_{AA}'s in low-p_T region ($p_T \lesssim 2$ GeV/c), where the hydrodynamic component dominates, at η=0 and 2.2, are almost identical. This is due to the comparable time evolution of the parton density at η =0 and 2.2 in hydrodynamics as shown in Fig. 2. PYTHIA prediction reveals that the spectrum at low p_T is very similar within $\eta<2$ up to a factor of 30% in pp collisions as shown in Fig. 1. $R_{AA}(\eta=0)>R_{AA}(\eta=2.2)$ at high p_T is a consequence of the steeper slope at η=2.2 compared to the slope at η=0 in pQCD. When the p_T slope is steep, the nuclear modification factor becomes sensitive to nuclear effects: a small shift of a spectrum is likely to produce a large effect on the ratio of the shifted spectrum to the original one. It should be noted that, due to the above reason, the nuclear modification factor from the Cronin effect at SPS energies [46] is much larger than the one at RHIC energies [6–9]. The nuclear modification factor at η=3.25 in the range $p_T<5$ GeV/c is larger than at midrapidity, because thermalized parton density at η=3.25 is about 40% smaller than at midrapidity. However, $R_{AA}(\eta=3.25)$ eventually becomes smaller than the one for η=0 or 2.2 in the high-p_T region. This is due to the much steeper slope at high p_T.

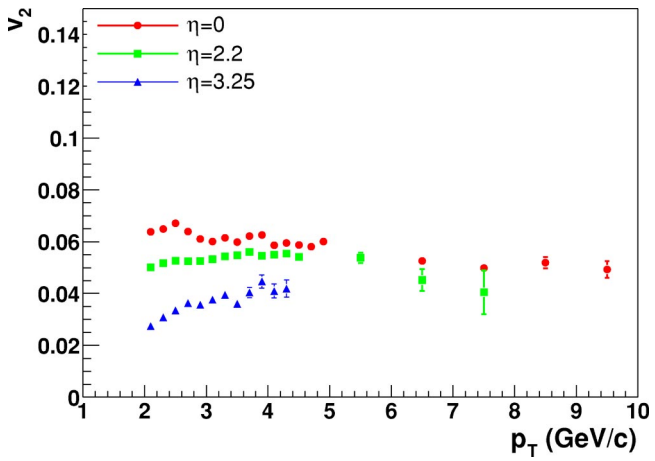

FIG. 5. (Color online) Elliptic flow parameter v_2 for charged hadrons at η=0, 2.2, and 3.25. The impact parameter is taken as b=7.2 fm. We only take into account contributions from hard components.

We also plot the ratio R_η defined by

$$R_\eta = \frac{R_{AA}(\eta = 2.2)}{R_{AA}(\eta = 0.0)}, \tag{4}$$

which can be compared with the data from BRAHMS defined by $R_\eta^{CP}=R_{CP}(\eta=2.2)/R_{CP}(\eta=0.0)$. Hydrodynamic predictions at very peripheral collisions are likely to be unreliable, since parton density is too small to justify the assumption of the local thermal system in Au+Au collisions at RHIC. In Fig. 4, R_η is found to be almost unity in low-p_T region and gradually decreases with p_T as consistent with data as expected in the above consideration.

One may worry about the nuclear shadowing effect on the R_η, since the accessible range of the parton momentum fraction x in the parton distribution functions at η=2.2 is smaller than at midrapidity. However, nuclear shadowing effect on $R_{AA}(\eta=2.2)<R_{AA}(\eta=0)$ is found to be ~15% around p_T =2–3 GeV/c within EKS98 parametrization. Other models for nuclear shadowing should be investigated elsewhere.

In order to disentangle the density effect from the "slope" effect among nuclear modification factors, we predict the elliptic flow parameter $v_2=\langle\cos(2\phi)\rangle$ for high-p_T charged hadrons in forward rapidity region as shown in Fig. 5. In this calculation, we only take account of the contributions from hard components. We choose the impact parameter as b =7.2 fm corresponding to 20–30% centrality. v_2 in high-p_T region is generated by jet quenching [25]. The difference of path length causes the difference of the amount of parton energy loss in azimuthal directions in noncentral collisions. Consequently, one can expect from Eq. (2) that the higher parton density results in the larger positive v_2 until v_2 reaches the limiting value [47]. As we expected, our prediction $v_2(\eta=3.25)<v_2(\eta=0)$ is a clear evidence of the density effect on the parton energy loss. We comment on our prediction on the v_2 at high $p_T>5$ GeV/c at midrapidity. Our prediction is similar to the results of the recent work [48] in which they found that the azimuthal anisotropy of high-p_T particles underestimates for a realistic nuclear density profile although hard-sphere nuclear profile looks consistent with the data [23].

In summary, we have studied the pseudorapidity dependence of the nuclear modification factors for charged hadrons within the hydro+jet model. In addition to the yield of charged hadrons, the radial flow at η_s=2 is found to be very similar to that at η_s=0. This results in $R_\eta\simeq 1$ at $p_T<2$ GeV/c. $R_\eta<1$ in high-p_T region can be understood by the steeper slope of p_T spectrum at η=2.2 than at η=0 from the pQCD components. This suggests that the longitudinal region of dense partonic matter produced in Au+Au collisions reaches to $\eta_s\sim 2$ and that strong hadron suppression at off-midrapidity is consistent with the final state parton energy loss in the medium. This reminds us the previous analysis of pseudorapidity dependence of elliptic flow at the RHIC energy [30,31] in which elliptic flow can be reproduced by hydrodynamics only in the region $|\eta|\lesssim 2$. We also predicted the elliptic flow parameter v_2 for high-p_T charged hadrons in both midrapidity and forward rapidity regions. We found the strong rapidity dependence of $v_2(p_T)$.

It would be very interesting to see how robust the present results are in a more realistic analysis. For example, the lattice studies predict the nontrivial behavior of screening mass in the vicinity of phase transition region [49]. This affects the space-time evolution of the parton density in the energy loss formula in Eq. (2). The parton density is multiplied by the correction factor for the effective degree of freedom μ^2/μ_0^2 [50] where μ_0 and μ are, respectively, perturbative and nonperturbative screening masses. The reduction of energy loss due to the nonperturbative behavior of the screening mass is expected to be large in forward rapidity region where the initial parton density is not so large. This modification causes the change of equation of state (EOS) as well as the amount of the parton energy loss. Hence we may need to use different initial conditions and simulate the hydrodynamic model with a more realistic EOS. This is beyond the scope of this paper, although it should be revisited elsewhere.

The work of T.H. was supported by RIKEN. Y.N.'s research was supported by the DOE under Contract No. DE-FG03-93ER40792.

[1] K. Adcox *et al.*, PHENIX Collaboration, Phys. Rev. Lett. **88**, 022301 (2002).
[2] S. S. Adler *et al.*, PHENIX Collaboration, Phys. Rev. Lett. **91**, 072301 (2003).
[3] C. Adler *et al.*, STAR Collaboration, Phys. Rev. Lett. **89**, 202301 (2002).
[4] J. Adams *et al.*, STAR Collaboration, Phys. Rev. Lett. **91**, 172302 (2003).

[5] K. Adcox *et al.*, PHENIX Collaboration, Phys. Lett. B **561**, 82 (2003).
[6] S. S. Adler *et al.*, PHENIX Collaboration, Phys. Rev. Lett. **91** 072303 (2003).
[7] J. Adams *et al.*, STAR Collaboration, Phys. Rev. Lett. **91**, 072304 (2003).
[8] B. B. Back *et al.*, PHOBOS Collaboration, Phys. Rev. Lett. **91**, 072302 (2003).
[9] I. Arsene *et al.*, BRAHMS Collaboration, Phys. Rev. Lett. **91**, 072305 (2003).
[10] M. Gyulassy and M. Plümer, Phys. Lett. B **243**, 432 (1990); X.-N. Wang and M. Gyulassy, Phys. Rev. Lett. **68**, 1480 (1992); M. Gyulassy and X.-N. Wang, Nucl. Phys. **B420**, 583 (1994); X.-N. Wang, M. Gyulassy, and M. Plümer, Phys. Rev. D **51**, 3436 (1995).
[11] X. N. Wang, nucl-th/0307036.
[12] M. Gyulassy, I. Vitev, X. N. Wang, and B. W. Zhang, nucl-th/0302077.
[13] C. Adler *et al.*, STAR Collaboration, Phys. Rev. Lett. **90**, 082302 (2003).
[14] C. Adler *et al.*, STAR Collaboration, Phys. Rev. Lett. **90**, 032301 (2003); J. Adams *et al.*, STAR Collaboration, nucl-ex/0306007.
[15] S. S. Adler *et al.*, PHENIX Collaboration nucl-ex/0305013.
[16] R. Baier, Y. L. Dokshitzer, S. Peigné, and D. Schiff, Phys. Lett. B **345**, 277 (1995); R. Baier, Y. L. Dokshitzer, A. H. Mueller, S. Peigné, and D. Schiff, Nucl. Phys. **B484**, 265 (1997); R. Baier, Y. L. Dokshitzer, A. H. Mueller, and D. Schiff, Phys. Rev. C **58**, 1706 (1998); R. Baier, D. Schiff, and B. G. Zakharov, Annu. Rev. Nucl. Part. Sci. **50**, 37 (2000).
[17] U. A. Wiedemann, Nucl. Phys. **B588**, 303 (2000).
[18] B. G. Zakharov, Pis'ma Zh. Eksp. Teor. Fiz. **63**, 906 (1996) [JETP Lett. **63**, 952 (1996)].
[19] M. Gyulassy, P. Lévai, and I. Vitev, Nucl. Phys. **B594**, 371 (2001); **B571**, 197 (2000); Phys. Rev. Lett. **85**, 5535 (2000).
[20] I. Vitev and M. Gyulassy, Phys. Rev. Lett. **89**, 252301 (2002).
[21] S. y. Jeon, J. Jalilian-Marian, and I. Sarcevic, Phys. Lett. B **562**, 45 (2003); Nucl. Phys. **A723**, 467 (2003).
[22] T. Hirano and Y. Nara, Phys. Rev. C **66**, 041901(R) (2002).
[23] X. N. Wang, nucl-th/0305010.
[24] T. Hirano and Y. Nara, Phys. Rev. Lett. **91**, 082301 (2003).
[25] X. N. Wang, Phys. Rev. C **63**, 054902 (2001); M. Gyulassy, I. Vitev, and X. N. Wang, Phys. Rev. Lett. **86**, 2537 (2001).
[26] M. Gyulassy, I. Vitev, X. N. Wang, and P. Huovinen, Phys. Lett. B **526**, 301 (2002).
[27] T. Hirano and Y. Nara, nucl-th/0307015.
[28] T. Hirano and Y. Nara, nucl-th/0211096.
[29] See, for example, P. Huovinen, nucl-th/0305064; P. F. Kolb and U. Heinz, nucl-th/0305084.
[30] T. Hirano, Phys. Rev. C **65**, 011901 (2002).
[31] T. Hirano and K. Tsuda, Phys. Rev. C **66**, 054905 (2002).
[32] J. D. Bjorken, Phys. Rev. D **27**, 140 (1983).
[33] J. H. Lee (unpublished); see also, http://www4.rcf.bnl.gov/brahms/WWW/presentations/2003/RHICAGSUsersMeeting03.pdf
[34] I. G. Bearden *et al.*, BRAHMS Collaboration, Phys. Rev. Lett. **88**, 202301 (2002).
[35] B. B. Back *et al.*, PHOBOS Collaboration, Phys. Rev. Lett. **87**, 102303 (2001).
[36] B. B. Back *et al.*, PHOBOS Collaboration, Phys. Rev. Lett. **89**, 222301 (2002).
[37] Y. Akase, M. Mizutani, S. Muroya, M. Namiki, and M. Yasuda, Prog. Theor. Phys. **85**, 305 (1991).
[38] T. Sjostrand, P. Eden, C. Friberg, L. Lonnblad, G. Miu, S. Mrenna, and E. Norrbin, Comput. Phys. Commun. **135**, 238 (2001).
[39] H. L. Lai *et al.*, CTEQ Collaboration, Eur. Phys. J. C **12**, 375 (2000).
[40] S. S. Adler *et al.*, PHENIX Collaboration, hep-ex/0304038.
[41] C. Albajar *et al.*, UA1 Collaboration, Nucl. Phys. **B335**, 261 (1990).
[42] K. J. Eskola, V. J. Kolhinen, and P. V. Ruuskanen, Nucl. Phys. **B535**, 351 (1998); K. J. Eskola, V. J. Kolhinen, and C. A. Salgado, Eur. Phys. J. C **9**, 61 (1999).
[43] X. N. Wang, Phys. Rev. C **61**, 064910 (2000); Phys. Lett. B **565**, 116 (2003).
[44] Parton density $\rho(\tau, \boldsymbol{x})$ from our full 3D hydrodynamic simulation used in this paper and Refs. [24,27] can be downloaded from the web (http://quark.phy.bnl.gov/~hirano/hydrodata/par_evo.html). The package includes a sample FORTRAN program which calls local parton density, temperature, and transverse velocity in the QGP phase.
[45] We note that the initial conditions in which there is no flat region in longitudinal directions can also give the same amount of pseudorapidity density at $\eta \lesssim 2$: T. Hirano and Y. Nara, (unpublished).
[46] M. M. Aggarwal *et al.*, WA98 Collaboration, Eur. Phys. J. C **23**, 225 (2002).
[47] E. V. Shuryak, Phys. Rev. C **66**, 027902 (2002).
[48] A. Drees, H. Feng, and J. Jia, nucl-th/0310044.
[49] See, for example, O. Kaczmarek, F. Karsch, E. Laermann, and M. Lutgemeier, Phys. Rev. D **62**, 034021 (2000).
[50] R. D. Pisarski, hep-ph/0203271; A. Dumitru and R. D. Pisarski, Phys. Lett. B **525**, 95 (2002); Nucl. Phys. **A698**, 444 (2002).